Author Manuscript

Author Manuscript

Author Manuscript

Author Manuscript

HHS Public Access

Author manuscript

*Arch Toxicol*. Author manuscript; available in PMC 2017 October 26.

Published in final edited form as:

*Arch Toxicol*. 2013 June ; 87(6): 1075–1086. doi:10.1007/s00204-012-0938-8.

# Size influences the cytotoxicity of poly (lactic-co-glycolic acid) (PLGA) and titanium dioxide ($TiO_2$) nanoparticles

**Sijing Xiong**,
School of Materials Science and Engineering, Nanyang Technological University, Block N4.1, 50 Nanyang Avenue, Singapore 639798, Singapore

**Saji George**,
California NanoSystems Institute, University of California, Los Angeles, CA 90095, USA

Centre for Sustainable Nanotechnology, School of Chemical and Life Sciences, Nanyang Polytechnic, Singapore 569824, Singapore

**Haiyang Yu**,
School of Materials Science and Engineering, Nanyang Technological University, Block N4.1, 50 Nanyang Avenue, Singapore 639798, Singapore

**Robert Damoiseaux**,
California NanoSystems Institute, University of California, Los Angeles, CA 90095, USA

**Bryan France**,
California NanoSystems Institute, University of California, Los Angeles, CA 90095, USA

**Kee Woei Ng**, and
School of Materials Science and Engineering, Nanyang Technological University, Block N4.1, 50 Nanyang Avenue, Singapore 639798, Singapore

**Joachim Say-Chye Loo**
School of Materials Science and Engineering, Nanyang Technological University, Block N4.1, 50 Nanyang Avenue, Singapore 639798, Singapore

## Abstract

The aim of this study is to uncover the size influence of poly (lactic-co-glycolic acid) (PLGA) and titanium dioxide ($TiO_2$) nanoparticles on their potential cytotoxicity. PLGA and $TiO_2$ nanoparticles of three different sizes were thoroughly characterized before in vitro cytotoxic tests which included viability, generation of reactive oxygen species (ROS), mitochondrial depolarization, integrity of plasma membrane, intracellular calcium influx and cytokine release. Size-dependent cytotoxic effect was observed in both RAW264.7 cells and BEAS-2B cells after cells were incubated with PLGA or $TiO_2$ nanoparticles for 24 h. Although PLGA nanoparticles did not trigger significantly lethal toxicity up to a concentration of 300 μg/ml, the TNF-α release after the stimulation of PLGA nanoparticles should not be ignored especially in clinical applications. Relatively more toxic $TiO_2$ nanoparticles triggered cell death, ROS generation,

Correspondence to: Joachim Say-Chye Loo.

**Conflict of interest** The authors declare that they have no conflict of interest.

Author Manuscript Author Manuscript Author Manuscript Author Manuscript

mitochondrial depolarization, plasma membrane damage, intracellular calcium concentration increase and size-dependent TNF-α release, especially at a concentration higher than 100 μg/ml. These cytotoxic effects could be due to the size-dependent interaction between nanoparticles and biomolecules, as smaller particles tend to adsorb more biomolecules. In summary, we demonstrated that the ability of protein adsorption could be an important paradigm to predict the in vitro cytotoxicity of nanoparticles, especially for low toxic nanomaterials such as PLGA and $TiO_2$ nanoparticles.

**Keywords**

PLGA; $TiO_2$; Nanoparticles; Cytotoxicity; Nanotoxicity; Protein adsorption

## Introduction

The safety of nanomaterials is receiving more and more attention in this decade (Oberdörster et al. 2005b; Nel et al. 2006), because products based on nanotechnology have penetrated into our daily lives, ranging from cosmetics to medical products (McCall 2011; Nel et al. 2006). However, more attention is paid to soluble metal oxide particles, such as ZnO, that release toxic metal ions like $Zn^{2+}$ (George et al. 2009; Ng et al. 2011; Heng et al. 2010a, b). The potential mechanism of cytotoxicity induced by non-soluble metal oxide such as titanium dioxide ($TiO_2$) nanoparticles and biomedical nanomaterials is still controversial. $TiO_2$ nanoparticles are even considered as a “natural” nanomaterial and are positively accepted by the general public (Skocaj et al. 2011). However, some reports have pointed out the potential toxicity of $TiO_2$ nanoparticles, including their ability to induce oxidative stress (Gurr et al. 2005; Kang et al. 2008; Long et al. 2006; Park et al. 2008), genotoxicity (Petkovic et al. 2010; Rahman et al. 2002; Wang et al. 2007), and immunotoxicity (Sayes et al. 2006; Palomaki et al. 2009). However, the mechanism behind these cytotoxic effects is still unclear. Besides these nonsoluble metal oxide particles, more attention should also be given to biomedical nanomaterials. Zhao et al. (2010) reported that hydroxyapatite (HA) nanoparticles of three different surface areas did not cause significant decrease in cell viability, but higher ROS generation was observed in the cells after incubating with HA nanoparticles of large surface areas. Poly (lactic-co-glycolic acid) (PLGA) nanoparticles are also widely studied for biomedical applications and have great potential to be used in drug delivery systems. The encapsulation of drugs into PLGA nanoparticles can prevent premature drug degradation, reduce side effects, enhance drug efficacy, achieve desired drug release rates, etc. (Dong and Feng 2007; Cartiera et al. 2009). Although more than 1,000 articles, on PLGA nanoparticle as drug delivery systems have been published and indexed in the Web of Science, the number of papers with that reports on its cytotoxicity are fewer than 10. Thus, it is crucial to understand the potential toxicity and cytotoxic mechanism of these nanomaterials. Since the toxicity of nanoparticles is related to their physicochemical properties such as size, shape, chemical composition, surface area, surface chemistry, surface charge, etc. (Oberdörster et al. 2005a), understanding how these properties can influence cytotoxicity will provide us with useful insights on the possible mechanisms behind their toxicity.

Author Manuscript Author Manuscript Author Manuscript Author Manuscript

The objective of this study is therefore to investigate the potential cytotoxicity of PLGA and $TiO_2$ nanoparticles, and how particle size can influence this outcome. Three different-sized PLGA and $TiO_2$ nanoparticles were investigated. RAW264.7 (murine macrophage) cells were chosen to represent the phagocytic cell lines, which can actively interact with foreign particles in in vivo systems (Xia et al. 2008; Zhao et al. 2010). BEAS-2B (human bronchial epithelial) cells were chosen to represent airway epithelium that is one of the defensive cells against inhaled nanoparticles (Zhao et al. 2010). RAW264.7 and BEAS-2B cells are well-understood cell line models for nanotoxicology studies (Xia et al. 2008; George et al. 2009; Zhao et al. 2012). We chose these two cell lines to evaluate and understand the cytotoxicity of different-sized PLGA and $TiO_2$ nanoparticles in order to compare our results with earlier studies. Moreover, in our previous studies, we have successfully used these two cell lines to investigate the cytotoxicity of different surface area of hydroxyapatite (HA) nanoparticles with potential biomedical applications (Zhao et al. 2010). Nanoparticles were characterized for their physicochemical properties before in vitro cytotoxicity studies. Cytotoxicity parameters tested included cell viability, generation of ROS, mitochondrial depolarization, plasma membrane leakage, increased intracellular calcium concentration and inflammation response. A potential paradigm to explain and predict the cytotoxicity of different-sized nanoparticles is proposed in this study.

## Materials and methods

### Materials

PLGA (RG502H) was purchased from Boehringer Ingelheim, Germany. PVA of molecular weight 30,000–70,000, acetone, dichloromethane (DCM) were purchased from Sigma-Aldrich, Singapore. The $TiO_2$ nanoparticles of different sizes were purchased from commercial sources. 10 nm (T10), 20 nm (T20) and 100 nm (T100) $TiO_2$ nanoparticles were purchased from SkySpring Nanomaterials Inc., Evonik Industries and MKnano Inc., respectively. PYROGENT® Plus single-test with CSE 0.06 EU/ml sensitivity (N289-06) was purchased from Lonza, Singapore. Bronchial epithelial cell growth medium (BEGM) (cc-3171 and cc-4175) was purchased from Lonza, USA. RAW264.7 (# TIB-71) cells and BEAS-2B (# CRL-9609) cells were purchased from ATCC, USA. Sodium pyruvate and penicillin-streptomycin were purchased from Hyclone, USA. Fetal bovine serum (FBS) was from Benchmark, USA. Dulbecco's modified eagle medium (DMEM), Hoechst (H3570), MitoSOX (M36008), JC-1 (T3168), propidium iodide (PI) nucleic acid stain (P3566) and Fluo-4 (F14202) were purchased from Invitrogen, USA. Mouse TNF-α ELISA (#430902) was purchased from Biolegend, Singapore. Pierce 660 nm Protein Assay (#22660) was purchased from Thermo Fisher Scientific, Singapore.

### Synthesis of PLGA nanoparticles

The PLGA nanoparticles were synthesized in house. The smallest PLGA nanoparticles (60 nm, P60) were synthesized through modified nanoprecipitation method (Chorny et al. 2002). In brief, 25 mg PLGA was dissolved in 6 ml of organic solvent mixture (acetone/DCM, 39:1, v/v). The PLGA solution was drop-wisely added into 18 ml 0.125 % PVA solution under magnetic stirring at 990 rpm. The organic solvent was removed through magnetically stirring for 24 h. The final colloid was freeze-dried for 48 h.

Author Manuscript Author Manuscript Author Manuscript Author Manuscript

The 100 and 200 nm PLGA nanoparticles (P100 and P200) were synthesized through modified oil in water (o/w) single emulsion solvent evaporation process (Song et al. 2008) using different organic solvent. In brief, 50 mg PLGA was dissolved in 1.5 ml organic solvent or solvent mixture. For P100, the organic solvent mixture composed of DCM and acetone (2/1, v/v). For P200, the organic solvent was chloroform only. 4.5 ml of PVA (1 %, w/v) solution was slowly added into the PLGA solution. Microtip probe ultrasonicator (Sonics & materials Inc., USA) was used to ultrasonicate the solution at the oil/water interface with ice water bath for 3 min. The organic solvent was removed through magnetically stirring for 24 h. The final colloid was freeze-dried for 48 h.

## Characterization of nanoparticles

**Size and zeta potential measurement—**The primary particle sizes of the PLGA and $TiO_2$ nanoparticles were characterized by using field emission scanning electron microscope (FESEM, Jeol JSM 6340F) and transmission electron microscope (TEM, JOEL 2010), respectively. The dispersed PLGA colloid in water was dropped onto a silica chip and air dried. The silica chip with PLGA nanoparticles was coated with platinum at 20 mA for 70 s under vacuum. The images were taken by using FESEM at an acceleration voltage of 2 kV. The dispersed $TiO_2$ nanoparticles in methanol were dropped onto a carbon-coated copper grids. The $TiO_2$ nanoparticles were observed under TEM at an accelerating voltage of 200 kV. The particle size was measured by using ImageJ software.

The hydrodynamic size and zeta potential of the particles in water, complete Dulbecco's modified eagle medium (CDMEM) and bronchial epithelial growth medium (BEGM), were measured by using dynamic light scattering (DLS) technique. The stock suspension (3 mg/ml) of nanoparticles was prepared by dispersing the particle powder in deionized water, CDMEM or BEGM. Ultrasonication was conducted in water bath ultrasonicator for 10 min. The colloid was diluted into working suspension at a concentration of 30 μg/ml. The working suspension was ultrasonicated for another 10 min before testing with ZetaPALS zeta potential analyzer (Brookhaven instruments, USA).

**Brunauer Emmett Teller (BET) surface area and theoretical surface area—**The specific surface area of $TiO_2$ nanoparticles was tested by using the Brunauer Emmett Teller (BET) method. The $TiO_2$ powder was degassed for 4 h at 200 °C in flowing nitrogen prior to nitrogen absorption using Micromeritics surface area analyzer (ASAP 2000, USA).

The theoretical surface area was calculated through Eq. (1) (Jang et al. 2001).

$$S=6/\rho d \quad (1)$$

$S$ represents the theoretical surface area. $\rho$ is the true density of materials. $d$ represents the mean diameter of nanoparticles. The true density of PLGA and $TiO_2$ was estimated at 1.357 $g/cm^3$ (Duvvuri et al. 2005) and 3.900 $g/cm^3$ (Tanaka and Suganuma 2001), respectively.

**X-ray powder diffraction (XRD) test—**The crystal structure of three different-sized $TiO_2$ nanoparticles was investigated by XRD (Panalytical X'Pert Prodiffractometer, CuKα

Author Manuscript Author Manuscript Author Manuscript Author Manuscript

radiation). The step size was 0.02° and the counting time was 0.5 s/step over a range of 20°–80° 2$\theta$.

## In vitro cell culture study

**Cell culture—**RAW264.7 cells were cultured in CDMEM containing 88 % DMEM, 10 % FBS, 1 % sodium pyruvate and 1 % penicillin-streptomycin. BEAS-2B cells were cultured in BEGM. The cells were sub-cultured at 70–80 % confluence about every 3 days and incubated in a humidified atmosphere containing 5 % $CO_2$ at 37 °C.

**Cell metabolic activity study—**RAW264.7 and BEAS-2B cells were seeded in 96-well plate and incubated for 24 h before nanoparticles of different concentrations were added. The cells were incubated with nanoparticles for another 24 h. After the incubation period, the supernatant medium was collected for TNF-α measurement using ELISA (see below). The cells were added with MTS working solution in complete cell culture medium and incubated for 1 h. The whole 96-well plate was centrifuged at 250 g for 10 min in order to spin down nanoparticles that could interfere with the absorbance reading. The supernatant was collected to measure the absorbance at 490 nm using SpectraMax M5e (Molecular Devices Corporation, USA). The absorbance at 690 nm was used as reference.

**Multiparametric assay—**Cytotoxicity parameters including ROS generation, mitochondrial depolarization, plasma membrane leakage and increased intracellular calcium concentration were tested using high throughput screening platform (George et al. 2009). Three sets of fluorescence probe cocktails were prepared by mixing wavelength-compatible fluorescent probes in PBS. The first cocktail contained 1 μM Hoechst (blue) and 5 μM MitoSOX (red). The second cocktail contained 1 μM Hoechst (blue) and 1 μM JC-1 (red/green). The third cocktail contained 1 μM Hoechst (blue), 5 μM propidium iodide (PI) (red) nucleic acid stain and 5 μM Fluo-4 (green). The use of different probes to track cellular responses is summarized in Table 1. Cells were seeded in 384-well plate with transparent bottom and incubated for 24 h to allow attachment. Nanoparticles of different concentrations were added and incubated with cells for another 24 h. On the third day, cells were washed twice with PBS, and then incubated with 25 μl dye cocktail in the dark for 30 min in 37 °C with humidified atmosphere containing 5 % $CO_2$. The fluorescent images were taken automatically using an automated epifluorescence microscope, Image-Xpress$^{mcro}$ (Molecular Devices, Sunnyvale, USA) under 10× magnifications. The images were automatically analyzed by using Meta-Xpress software to calculate the percentage of cells showing positive signals.

**ELISA test for TNF-α and endotoxin test—**The TNF-α released into the medium was measured by Mouse TNF-α ELISA following the protocol provided by Biolegend. To exclude the possibility that the inflammation response of cells was due to the stimulation by endotoxin attached on materials, the endotoxin level in nanoparticle samples was tested using PYROGENT® Plus single-test with CSE 0.06 EU/ml sensitivity following the protocol provided by Lonza. The endotoxin test was conducted for all nanoparticles at a concentration of 300 μg/ml.

Author Manuscript Author Manuscript Author Manuscript Author Manuscript

**Nanoparticle-protein adsorption study—**Nanoparticles (1 mg/ml) were dispersed in 2 mg/ml bovine serum albumin (BSA) in DMEM solution and ultrasonicated for 20 min. All the particles were collected by centrifugation at 14,000 rpm for 20 min at 25 °C and washed thrice with Milli-Q water. The protein attached on PLGA nanoparticles was quantified using Pierce 660 nm Protein Assay following the manufacture's protocol using Bovine Serum Albumin (BSA) as a model protein. The adsorption of protein on $TiO_2$ nanoparticles was tested using Thermo Gravimetric Analyzer (TGA, 2950, HR, V5.4A). The collected $TiO_2$ nanoparticles were freeze-dried for 48 h before the TGA test. The curves of weight loss for BSA and BSA adsorbed $TiO_2$ nanoparticles were obtained at a heating rate of 20 °C/min in a nitrogen-filled atmosphere.

### Statistics

All quantitative data are shown as the mean ± standard deviation (SD). Statistical analysis was conducted by using a one-way analysis of variance (ANOVA) and Tukey's pairwise comparisons. The difference was considered to be significant when $p < 0.05$. * represented the data with significant difference when it is compared with the control group. # represented the data with significant difference when it is compared with other particles at the same concentration. All tests were repeated four times.

## Results and discussion

### Physical characterization of PLGA and $TiO_2$ nanoparticles

The characterization data for the particles tested are listed in Table 2. Their SEM and TEM images are shown in Fig. 1, which reflect the primary size and morphology of PLGA and $TiO_2$ nanoparticles. The PLGA nanoparticles of three different sizes were spherical with a mean diameter of 61 nm for P60 (a), 94 nm for P100 (b) and 205 nm for P200 (c), which was measured using the SEM images. The $TiO_2$ nanoparticles of three different sizes were nearspherical particles with primary size 10 nm for T10 (d), 20 nm for T20 (e) and 100 nm (f) for T100 as shown in Fig. 1. DLS technique was used to measure the hydrodynamic size and zeta potential of the nanoparticles in both water and complete cell culture medium CDMEM and BEGM (Table 2). The hydrodynamic size was bigger than their primary size. Although different particles showed different surface charge in water, the zeta potentials in CDMEM and BEGM were similar within the range of −2 to −13 mV. This could be due to the adsorption of the proteins and ions in the cell culture medium onto the particle surface, resulting in the neutralization of surface charge (Xia et al. 2006). The BET method was utilized to quantify the specific surface area of $TiO_2$ nanoparticles. However, this method was not applicable for PLGA nanoparticles due to the low melting point of PLGA polymer. From the results shown in Table 2, the smallest $TiO_2$ nanoparticles (T10) had the highest BET surface area (166.0 $m^2/g$). The experimental BET surface area was close to the theoretical surface areas calculated through the size and true density of the materials (Eq. 1). These results indicated that smaller particles had larger surface areas. The crystal structure of $TiO_2$ nanoparticles were tested through XRD. Results show that $TiO_2$ nanoparticles of three different sizes were mainly anatase. The endotoxin test was conducted to exclude the possibility that the inflammation response of the cells was due to the endotoxin attached on the materials. From Table 2, the endotoxin in the materials was lower than 0.06 EU/ml at the

Author Manuscript Author Manuscript Author Manuscript Author Manuscript

highest particle concentration of 300 μg/ml. This result suggested that the inflammation response of the cells could be more likely due to the particles themselves instead of the endotoxin in the samples.

### Limited effect of PLGA and $TiO_2$ nanoparticles on cell viability

To test the cytotoxicity of PLGA and $TiO_2$ nanoparticles, the particles of concentrations ranging from 10 to 300 μg/ml were incubated with RAW264.7 and BEAS-2B cells for 24 h. For in vitro cell viability test, MTS assay was utilized to quantify the metabolically active cells through the interaction between MTS and dehydrogenase enzymes in live cells. Figure 2 exhibited the metabolic activity of cells after interaction with PLGA (a and b) and $TiO_2$ (c and d) nanoparticles. The graph indirectly indicates the viability of live cells in each group as compared with the negative control (0 μg/ml). Figure 2a, b showed no apparent cytotoxicity for PLGA nanoparticles regardless of the size. This result is consistent with other reports that PLGA nanoparticles do not show obvious acute lethal toxicity to cells within 24 h of incubation (de Lima et al. 2011; Semete et al. 2010). As for $TiO_2$ nanoparticles, cell viability was generally uncompromised (>80 %) after 24 h exposure (Fig. 2c, d). However, viability of BEAS-2B cells was statistically lower after they were exposed to 300 mg/ml of T10 and T20 nanoparticles as compared with the negative control (Fig. 2d).

### Cells displayed different responses to different-sized nanoparticles in the multiparametric assay

There are many biological and molecular reactions happening in cells upon stimulation with nanoparticles (Oberdörster et al. 2005b; Nel et al. 2006). Among them, the oxidative stress stimulated by nanoparticles is considered a useful paradigm to predict the toxicity of nanomaterials (Xia et al. 2006). Oxidative stress could trigger a range of oxidant injuries including mitochondrial depolarization, intracellular calcium ion influx and even cause the death of cells (George et al. 2009). George et al. (2009) showed that the cytotoxicity events involved in oxidative stress pathway could be measured using fluorescence probes. These dyes were Hoechst, PI, MitoSOX, JC1 and Fluo-4 (George et al. 2009, 2011; Zhang et al. 2011). Hoechst and PI are the two DNA interactive agents. The cell-permeable Hoechst is utilized to bind to DNA of both live and dead cells, allowing us to quantify and locate the total cells in each image. The PI can only penetrate into dead cells through the damaged plasma membrane to indicate the number of dead cells (George et al. 2009). The generation of superoxide in mitochondria can be detected with MitoSOX Red staining. If ROS generation causes oxidative stress in cells, a decrease in mitochondrial membrane potential would be detected using cationic dye JC1, which indicates unhealthy mitochondria (George et al. 2009). JC1 is normally accumulated in the mitochondria of healthy cells. But during mitochondrial depolarization, the dye is released from the mitochondria to the cytosol. This release will cause the fluorescence color to shift from red to green, which forms the basis of quantifying cells with decreased mitochondrial potential. Fluo-4 is a dye to detect intracellular calcium levels, which fluoresces green when there is an increase in the intracellular calcium ions.

This multiparametric assay was conducted after RAW264.7 and BEAS-2B cells were exposed to differentsized nanoparticles for 24 h. The results shown in Figs. 3, 4 indicated the

Author Manuscript Author Manuscript Author Manuscript Author Manuscript

percentage of positive cells for each parameter whose fluorescence intensity was above a certain threshold using Meta-Xpress software. The potential cytotoxic effects of PLGA nanoparticles were shown in Fig. 3. Limited damaging response was observed in both of RAW264.7 and BEAS-2B cells after incubation with PLGA nanoparticles (positive cells <10 %). However, the smallest PLGA nanoparticles (P60) triggered similar increase in the intracellular calcium flux in both RAW264.7 and BEAS-2B cells. Calcium is an important regulator of mitochondrial function. The disturbance of cytosolic calcium homeostasis may trigger profound influence on cell functions (Brookes et al. 2004). High concentration of $Ca^{2+}$, especially in pathology, has negative effect on the function of mitochondria through ROS generation (Brookes et al. 2004). But based on our current results, the slight increase in the calcium concentration in P60 treated cells did not cause obvious cell death or damage of organelles. The $TiO_2$ nanoparticles exhibited more obvious size and concentration-dependent cytotoxicity to both RAW264.7 and BEAS-2B cells (Fig. 4). The PI uptake results confirmed the results in MTS tests that only T10 and T20 triggered ~ 10 % cell death at the highest concentration of 300 μg/ml. Size-dependent generation of mitochondrial superoxide was observed in both RAW264.7 and BEAS-2B cells. ROS generation after the interaction with $TiO_2$ nanoparticles in the in vitro studies was also observed in BEAS-2B cells by other groups (Wang et al. 2007; Gurr et al. 2005). Only T10 triggered statistically increased signal in intracellular calcium flux parameter in both RAW264.7 and BEAS-2B cells at the concentration higher than 100 μg/ml. In summary, the results of the multiparametric assay showed that the cytotoxicity of PLGA and $TiO_2$ nanoparticles was size dependent and smaller particles tend to trigger higher level of damage to both RAW264.7 and BEAS-2B cells in this in vitro investigation.

## PLGA and $TiO_2$ nanoparticles triggered size and concentration-dependent inflammation response

Nanoparticles have different ways of entering the human body and activating the immune system. PLGA nanoparticles, proposed to be used in biomedical field, were designed to deliver drugs through intravenous administration. As for $TiO_2$ nanoparticles, although they are more commonly used in sunscreens, they still have great potential to enter human body through lung and gastrointestinal tract (Skocaj et al. 2011). The immune systems in living organisms have many ways to protect themselves from the attacks by “foreign invaders”, which include infectious bacteria, virus as well as natural and synthetic materials (Sim and Wallis 2011). The expression of proinflammatory cytokines such as TNF-α released from macrophages can be used to indicate the inflammatory responses. TNF-α plays an active role in mediating inflammation, generalized wasting and septic shock (Ziolli and Jardim 2002), programmed cell death (Ziolli and Jardim 2002) and metabolic disturbances in cancer patients (Zhang et al. 2007). TNF-α induction of cytokine cascades can induce and maintain inflammation. Although the evolutionary advantages of inflammatory response could be the resistance to infection, the unnecessary and prolonged inflammation may cause damages to human health. RAW264.7 cells, a kind of macrophage cells, can release cytokines such as TNF-α with the stimulation of materials in the earlier phase of inflammation (Ding et al. 2009). In this study, we tested the TNF-α released from RAW264.7 cells after 24 h incubation with PLGA and $TiO_2$ nanoparticles (Fig. 5). The graph showed an obvious trend that smaller particles tend to trigger more release of cytokine TNF-α from RAW264.7 cells.

Author Manuscript Author Manuscript Author Manuscript Author Manuscript

P60 and P100 nanoparticles started to show statistical difference when compared with control from 10 to 100 μg/ml, respectively. The P200 nanoparticles did not trigger significant release of TNF-α up to 300 μg/ml. This result indicated that PLGA nanoparticles with size larger than 100 nm would be safer for biomedical applications. As for $TiO_2$ nanoparticles, T10 triggered the highest level of cytokine release starting from 10 μg/ml. Both T20 and T100 triggered similar amount of TNF-α release, which showed statistical difference from the control at 100 μg/ml. The TNF-α release stimulated by $TiO_2$ nanoparticles was also observed by other studies (Palomaki et al. 2009; Tao and Kobzik 2002). $TiO_2$ could not only trigger the expression of TNF-α but also stimulate the release of other cytokines including IL-6 and MIP-1α from macrophages (Palomaki et al. 2009). The increase in maturation of macrophage and antigen presentation triggered by $TiO_2$ nanoparticles was also observed in Palomaki et al.'s (2009) study. Similar trend was also observed by Oberdorster et al. (1992) from their in vivo study whereby after intratracheal instillation of different-sized $TiO_2$ nanoparticles, obvious acute inflammatory response was indicated by the lung lavage parameters. This pulmonary inflammatory response correlated well with surface area of particles instead of particle mass, volume or numbers, so similarly smaller particles with higher surface area could also trigger higher level of inflammatory response.

### The protein adsorption on PLGA and $TiO_2$ nanoparticles was size dependent

All the cytotoxicity studies showed that the cytotoxicity of PLGA and $TiO_2$ nanoparticles was size dependent. Unlike other nanomaterials such as ZnO, PLGA and $TiO_2$ nanoparticles do not release toxic ions like $Zn^{2+}$. Thus, the potential mechanism behind this cytotoxicity could be due to the size-dependent interaction between nanoparticles and intracellular biomolecules adsorbed onto nanoparticles. Smaller nanoparticles have larger surface area and higher percentage of molecules exposed on particle surface to interact with surrounding biomolecules. To investigate this hypothesis, we studied the adsorption of BSA (a model biomolecule) to different-sized PLGA and $TiO_2$ nanoparticles. Two different methods, Pierce 660 test and TGA analysis, were chosen to test the protein adsorption onto PLGA nanoparticles and $TiO_2$ nanoparticles, respectively. This is because the $TiO_2$ nanoparticles have strong absorbance at 660 nm which interferes with the absorbance of Pierce 660 reagent. Meanwhile, the PLGA polymer is unstable for TGA analysis. Figure 6a shows the protein quantification of BSA attached on PLGA nanoparticles through Pierce 660 assay. The theoretical surface area of PLGA nanoparticles (per 100 mg) and the amount of BSA adsorbed onto 100 mg PLGA nanoparticles for P60, P100 and P200 were listed in the table of Fig. 6a. The protein adsorption correlated well with the surface area of the PLGA nanoparticles ($R^2 > 0.9$). Similar trend was also observed in Fig. 6b, which is the TGA result of BSA adsorption onto $TiO_2$ nanoparticles. The weight decreased more for T10-BSA and T20-BSA when compared with T100-BSA in the temperature range from 188 to 485 °C, which was the major weight loss temperature range of BSA protein. This indicated more BSA adsorbed onto T10 and T20 nanoparticles than on relatively larger T100 nanoparticles. By comparing the results in Fig. 6a, b, 100 mg of P100 nanoparticles could only adsorb 0.441 mg of BSA, but 100 mg of T100 nanoparticles could adsorb more than 2 mg of BSA. This could be the reason for the higher cytotoxicity of 100 nm $TiO_2$ nanoparticles as compared with 100 nm PLGA nanoparticles. BSA remained attached on these nanoparticles

Author Manuscript Author Manuscript Author Manuscript Author Manuscript

after extensive washing, which indicated a high-affinity interaction between BSA and nanoparticles especially for $TiO_2$ nanoparticles.

The data therefore suggest that the size-dependent cytotoxicity of PLGA and $TiO_2$ nanoparticles should be related to different surface area of different-sized nanoparticles. Smaller particles have bigger surface area and more molecules exposed on particle surface to interact with intracellular biomolecules nearby. The potential mechanism of such size-dependent cytotoxicity is shown in Fig. 7. When nanoparticles come in to contact with intracellular biomolecules, these biomolecules may adsorb onto the surface of the particles and interact with these “intruder” nanoparticles. These interactions may then trigger a series of responses in cells including generation of reactive oxygen species (ROS), mitochondrial depolarization, plasma membrane leakage, intracellular calcium influx and cytokine release.

Although it has been found that reaction between nanoparticles and proteins is related to some pathological changes such as protein aggregation or unfolding, the mechanism of these damages is still poorly investigated and understood (Deng et al. 2011). Some studies have reported that the interaction between nanoparticles and biomolecules could lead to dysfunction or damage of biomolecules (Deng et al. 2011; Wang et al. 2010; Shang et al. 2007; Teichroeb et al. 2008). Wang et al. (2010) investigated the interaction between $TiO_2$ nanoparticles and trypsin. They observed a strong physical adsorption effect of $TiO_2$ nanoparticles on enzyme trypsin and found inhibitory effect of $TiO_2$ nanoparticles on trypsin activity by changing the $\alpha$-helix and $\beta$-sheet ratio of the protein structure. Deng et al. (2011) found the interaction between poly (acrylic acid) coated gold nanoparticles and fibrinogens would induce the unfolding of protein fibrinogen, which resulted in the activation of Mac-1 reception and inflammation response. Smaller particles (5 nm) tended to bind more fibrinogen than bigger particles (20 nm), and the adsorption was proportional to the surface area of nanoparticles. Wang et al. (2009) reported a size-dependent toxicity of silica nanoparticles on cultured human embryonic kidney (HEK293) cells. Twenty nanometer $SiO_2$ nanoparticles were more toxic than 50 nm $SiO_2$ nanoparticles. The possible reason could be related to the depletion of glutathione (GSH, a tripeptide responsible for the homeostasis of free radicals in cells), resulting in the increase in ROS. Smaller particles with higher surface area tend to trigger higher level of GSH decrease in cells. Horie et al. (2009) showed similar results that smaller $TiO_2$ nanoparticles tend to adsorb more proteins and cause severe toxic effect to human keratinocyte HaCaT cells and human lung carcinoma A549 cells. However, their explanation was that the cytotoxicity of $TiO_2$ nanoparticles was due to the depletion of proteins in the cell culture medium. But based on our data, even 300 μg/ml of $TiO_2$ nanoparticles did not cause obvious decrease in proteins in the cell culture medium (data not shown here). So the size-dependent cytotoxicity of $TiO_2$ nanoparticles is less likely due to nutrient depletion. Instead, the adsorption, denaturalization or even the damage of biomolecules could be a more reasonable explanation.

Thus, our studies demonstrated that the particles size can influence the cytotoxicity of nanoparticles. Smaller particles tend to have higher cytotoxicity, as smaller particles have more molecules exposed on the surface of particles to interact with surrounding biomolecules such as proteins. The protein adsorption could be an important paradigm to predict the in vitro cytotoxicity of nanoparticles, especially for low toxic nanoparticles such

Author Manuscript Author Manuscript Author Manuscript Author Manuscript

as PLGA and $TiO_2$ nanoparticles. The identification of the intracellular biomolecules attached on PLGA and $TiO_2$ nanoparticles is a proposed study in the future. Understanding the interaction between biomolecules and specific nanoparticles will guide in vitro and in vivo studies to understand mechanism behind the toxicity of nanoparticles. These studies will have great potential to be utilized in the prediction of cytotoxicity of different nanoparticles in an abiotic condition.

## Conclusions

In this study, we observed size-dependent cytotoxicity of both PLGA and $TiO_2$ nanoparticles. Biomedical used PLGA nanoparticles did not exhibit strong cytotoxic effect when compared with $TiO_2$ nanoparticles but the potential of smaller PLGA nanoparticles to trigger the release of TNF-α should not be ignored, especially for clinical applications. Two hundred nanometer PLGA nanoparticles did not trigger any negative response from cells based on our current results, but more studies are still needed to evaluate the biocompatibility of PLGA nanoparticles before they can be used in human body. Higher cytotoxic effect was observed in cells treated with $TiO_2$ nanoparticles, especially at concentration higher than 100 μg/ml. The damages include generation of ROS, mitochondrial depolarization, plasma membrane leakage, increased intracellular calcium concentration and inflammation response. The size-dependent cytotoxicity of both PLGA and $TiO_2$ nanoparticles could be due to the fact that smaller particles with larger specific surface area could adsorb more biomolecules such as proteins in the environment. Thus, the ability to adsorb proteins could be an important paradigm to predict the in vitro cytotoxicity of nanoparticles, especially for low toxic nanoparticles such as PLGA and $TiO_2$ nanoparticles.

## Acknowledgments

Ms Xiong Sijing would like to acknowledge the Nanyang Technological University—Ian Ferguson Postgraduate Fellowship support for her research attachment to University of California, Los Angeles (UCLA). We thank Dr. Andre E. Nel and Dr. Tian Xian (UC Center for Environmental Implications of Nanotechnology) for their kind help in this study. Financial support from the following funding agencies (NMRC, A*STAR and NITHM) are also acknowledged: NMRC/EDG/0062/2009 and A*STAR Project No: 102 129 0098.

## References

Brookes PS, Yoon YS, Robotham JL, Anders MW, Sheu SS. Calcium, ATP, and ROS: a mitochondrial love-hate triangle. Am J Physiol-Cell Physiol. 2004; 287(4):C817–C833. DOI: 10.1152/ajpcell.00139.2004 [PubMed: 15355853]

Cartiera MS, Johnson KM, Rajendran V, Caplan MJ, Saltzman WM. The uptake and intracellular fate of PLGA nanoparticles in epithelial cells. Biomaterials. 2009; 30(14):2790–2798. [PubMed: 19232712]

Chorny M, Fishbein I, Danenberg HD, Golomb G. Lipophilic drug loaded nanospheres prepared by nanoprecipitation: effect of formulation variables on size, drug recovery and release kinetics. J Controlled Release. 2002; 83(3):389–400.

de Lima R, do Espirito Santo Pereira A, Porto R, Fraceto L. Evaluation of cyto- and genotoxicity of poly(lactide-co-glyco- lide) nanoparticles. J Polym Environ. 2011; 19(1):196–202.

Deng ZJ, Liang MT, Monteiro M, Toth I, Minchin RF. Nanoparticle-induced unfolding of fibrinogen promotes Mac-1 receptor activation and inflammation. Nat Nanotechnol. 2011; 6(1):39–44. DOI: 10.1038/nnano.2010.250 [PubMed: 21170037]

Author Manuscript Author Manuscript Author Manuscript Author Manuscript

Ding T, Sun J, Zhang P. Study on MCP-1 related to inflammation induced by biomaterials. Biomed Mater. 2009; 4(3):035005. [PubMed: 19439823]

Dong Y, Feng SS. Poly(D, L-lactide-co-glycolide) (PLGA) nanoparticles prepared by high pressure homogenization for paclitaxel chemotherapy. Int J Pharm. 2007; 342(1–2):208–214. DOI: 10.1016/j.ijpharm.2007.04.031 [PubMed: 17560058]

Duvvuri S, Janoria KG, Mitra AK. Development of a novel formulation containing poly(d, l-lactide-co-glycolide) microspheres dispersed in PLGA-PEG-PLGA gel for sustained delivery of ganciclovir. J Controlled Release. 2005; 108:282–293.

George S, Pokhrel S, Xia T, Gilbert B, Ji Z, Schowalter M, Rosenauer A, Damoiseaux R, Bradley KA, Mädler L, Nel AE. Use of a rapid cytotoxicity screening approach to engineer a safer zinc oxide nanoparticle through iron doping. ACS Nano. 2009; 4(1):15–29. DOI: 10.1021/nn901503q

George S, Xia T, Rallo R, Zhao Y, Ji Z, Lin S, Wang X, Zhang H, France B, Schoenfeld D, Damoiseaux R, Liu R, Lin S, Bradley KA, Cohen Y, Nel AE. Use of a high-throughput screening approach coupled with in vivo zebrafish embryo screening to develop hazard ranking for engineered nanomaterials. ACS Nano. 2011; 5(3):1805–1817. DOI: 10.1021/nn102734s [PubMed: 21323332]

Gurr J-R, Wang ASS, Chen C-H, Jan K-Y. Ultrafine titanium dioxide particles in the absence of photoactivation can induce oxidative damage to human bronchial epithelial cells. Toxicology. 2005; 213(1–2):66–73. [PubMed: 15970370]

Heng BC, Zhao X, Xiong S, Ng KW, Boey FY-C, Loo JS-C. Toxicity of zinc oxide (ZnO) nanoparticles on human bronchial epithelial cells (BEAS-2B) is accentuated by oxidative stress. Food Chem Toxicol. 2010a; 48(6):1762–1766. [PubMed: 20412830]

Heng BC, Zhao X, Xiong S, Ng KW, Boey FYC, Loo JSC. Cytotoxicity of zinc oxide (ZnO) nanoparticles is influenced by cell density and culture format. Arch Toxicol. 2010b; 85(6):695–704. DOI: 10.1007/s00204-010-0608-7 [PubMed: 20938647]

Horie M, Nishio K, Fujita K, Endoh S, Miyauchi A, Saito Y, Iwahashi H, Yamamoto K, Murayama H, Nakano H, Nanashima N, Niki E, Yoshida Y. Protein adsorption of ultrafine metal oxide and its influence on cytotoxicity toward cultured cells. Chem Res Toxicol. 2009; 22(3):543–553. DOI: 10.1021/tx800289z [PubMed: 19216582]

Jang HD, Kim S-K, Kim S-J. Effect of particle size and phase composition of titanium dioxide nanoparticles on the photocatalytic properties. J Nanopart Res. 2001; 3(2):141–147. DOI: 10.1023/a:1017948330363

Kang JL, Moon C, Lee HS, Lee HW, Park EM, Kim HS, Castranova V. Comparison of the biological activity between ultrafine and fine titanium dioxide particles in RAW 264.7 cells associated with oxidative stress. J Toxicol Environ Health Part A. 2008; 71(8):478–485. DOI: 10.1080/15287390801906675 [PubMed: 18338282]

Long TC, Saleh N, Tilton RD, Lowry GV, Veronesi B. Titanium dioxide (P25) produces reactive oxygen species in immortalized brain microglia (BV2): implications for nanoparticle neurotoxicity. Environ Sci Technol. 2006; 40(14):4346–4352. [PubMed: 16903269]

McCall MJ. Environmental, health and safety issues nanoparticles in the real world. Nat Nanotechnol. 2011; 6(10):613–614. [PubMed: 21979234]

Nel A, Xia T, Madler L, Li N. Toxic potential of materials at the nanolevel. Science. 2006; 311(5761):622–627. DOI: 10.1126/science.1114397 [PubMed: 16456071]

Ng KW, Khoo SPK, Heng BC, Setyawati MI, Tan EC, Zhao X, Xiong S, Fang W, Leong DT, Loo JSC. The role of the tumor suppressor p53 pathway in the cellular DNA damage response to zinc oxide nanoparticles. Biomaterials. 2011; 32(32):8218–8225. [PubMed: 21807406]

Oberdorster G, Ferin J, Gelein R, Soderholm SC, Finkelstein J. Role of the alveolar macrophage in lung injury—studies with ultrafine particles. Environ Health Perspect. 1992; 97:193–199. DOI: 10.2307/3431353 [PubMed: 1396458]

Oberdörster G, Maynard A, Donaldson K, Castranova V, Fitzpatrick J, Ausman K, Carter J, Karn B, Kreyling W, Lai D, Olin S, Monteiro-Riviere N, Warheit D, Yang H, Group ArftIRFRSINTSW. Principles for characterizing the potential human health effects from exposure to nanomaterials: elements of a screening strategy. Part Fibre Toxicol. 2005a; 2(1):8. [PubMed: 16209704]

Author Manuscript Author Manuscript Author Manuscript Author Manuscript

Oberdörster G, Oberdörster E, Oberdörster J. Nanotoxicology: an emerging discipline evolving from studies of ultrafine particles. Environ Health Perspect. 2005b; 113(7):823–839. DOI: 10.1289/ehp.7339 [PubMed: 16002369]

Palomaki J, Karisola P, Pylkkanen L, Savolainen K, Alenius H. Engineered nanornaterials cause cytotoxicity and activation on mouse antigen presenting cells. Toxicology. 2009; 267(1–3):125–131. DOI: 10.1016/j.tox.2009.10.034 [PubMed: 19897006]

Park E-J, Yi J, Chung K-H, Ryu D-Y, Choi J, Park K. Oxidative stress and apoptosis induced by titanium dioxide nanoparticles in cultured BEAS-2B cells. Toxicol Lett. 2008; 180(3):222–229. [PubMed: 18662754]

Petkovic J, Zegura B, Stevanovic M, Drnovsek N, Uskokovic D, Novak S, Filipic M. DNA damage and alterations in expression of DNA damage responsive genes induced by TiO(2) nanoparticles in human hepatoma HepG2 cells. Nanotoxicology. 2010; 5(3):341–353. DOI: 10.3109/17435390.2010.507316 [PubMed: 21067279]

Rahman Q, Lohani M, Dopp E, Pemsel H, Jonas L, Weiss DG, Schiffmann D. Evidence that ultrafine titanium dioxide induces micronuclei and apoptosis in Syrian hamster embryo fibroblasts. Environ Health Perspect. 2002; 110(8):797–800.

Sayes CM, Wahi R, Kurian PA, Liu Y, West JL, Ausman KD, Warheit DB, Colvin VL. Correlating nanoscale titania structure with toxicity: a cytotoxicity and inflammatory response study with human dermal fibroblasts and human lung epithelial cells. Toxicol Sci. 2006; 92(1):174–185. [PubMed: 16613837]

Semete B, Booysen L, Lemmer Y, Kalombo L, Katata L, Verschoor J, Swai HS. In vivo evaluation of the biodistribution and safety of PLGA nanoparticles as drug delivery systems. Nanomed Nanotechnol Biol Med. 2010; 6(5):662–671.

Shang W, Nuffer JH, Dordick JS, Siegel RW. Unfolding of ribonuclease A on silica nanoparticle surfaces. Nano Lett. 2007; 7(7):1991–1995. DOI: 10.1021/nl070777r [PubMed: 17559285]

Sim RB, Wallis R. Surface properties: immune attack on nanoparticles. Nat Nano. 2011; 6(2):80–81.

Skocaj M, Filipic M, Petkovic J, Novak S. Titanium dioxide in our everyday life; is it safe? Radiol Oncol. 2011; 45(4):227–247. DOI: 10.2478/v10019-011-0037-0 [PubMed: 22933961]

Song X, Zhao Y, Wu W, Bi Y, Cai Z, Chen Q, Li Y, Hou S. PLGA nanoparticles simultaneously loaded with vincristine sulfate and verapamil hydrochloride: systematic study of particle size and drug entrapment efficiency. Int J Pharm. 2008; 350(1–2):320–329. [PubMed: 17913411]

Tanaka Y, Suganuma M. Effects of heat treatment on photocatalytic property of sol-gel derived polycrystalline TiO2. J Sol-Gel Sci Technol. 2001; 22(1–2):83–89. DOI: 10.1023/a:1011268421046

Tao F, Kobzik L. Lung macrophage-epithelial cell interactions amplify particle-mediated cytokine release. Am J Respir Cell Mol Biol. 2002; 26(4):499–505. [PubMed: 11919087]

Teichroeb J, Forrest J, Jones L. Size-dependent denaturing kinetics of bovine serum albumin adsorbed onto gold nanospheres. Eur Phys J E: Soft Matter Biol Phys. 2008; 26(4):411–415. DOI: 10.1140/epje/i2007-10342-9

Wang JJ, Sanderson BJS, Wang H. Cyto- and genotoxicity of ultrafine TiO2 particles in cultured human lymphoblastoid cells. Mutat Res/Genet Toxicol Environ Mutagen. 2007; 628(2):99–106.

Wang F, Gao F, Lan M, Yuan H, Huang Y, Liu J. Oxidative stress contributes to silica nanoparticle-induced cytotoxicity in human embryonic kidney cells. Toxicol In Vitro. 2009; 23(5):808–815. [PubMed: 19401228]

Wang WR, Zhu RR, Xiao R, Liu H, Wang SL. The electrostatic interactions between nano-TiO(2) and trypsin inhibit the enzyme activity and change the secondary structure of trypsin. Biol Trace Elem Res. 2010; 142(3):435–446. DOI: 10.1007/s12011-010-8823-x [PubMed: 20809270]

Xia T, Kovochich M, Brant J, Hotze M, Sempf J, Oberley T, Sioutas C, Yeh JI, Wiesner MR, Nel AE. Comparison of the abilities of ambient and manufactured nanoparticles to induce cellular toxicity according to an oxidative stress paradigm. Nano Lett. 2006; 6(8):1794–1807. [PubMed: 16895376]

Xia T, Kovochich M, Liong M, Madler L, Gilbert B, Shi H, Yeh JI, Zink JI, Nel AE. Comparison of the mechanism of toxicity of zinc oxide and cerium oxide nanoparticles based on dissolution and

Author Manuscript Author Manuscript Author Manuscript Author Manuscript

oxidative stress properties. ACS Nano. 2008; 2(10):2121–2134. DOI: 10.1021/nn800511k [PubMed: 19206459]

Zhang N, Chittasupho C, Duangrat C, Siahaan TJ, Berkland C. PLGA nanoparticle-peptide conjugate effectively targets intercellular cell-adhesion molecule-1. Bioconjug Chem. 2007; 19(1):145–152. DOI: 10.1021/bc700227z [PubMed: 17997512]

Zhang H, Xia T, Meng H, Xue M, George S, Ji Z, Wang X, Liu R, Wang M, France B, Rallo R, Damoiseaux R, Cohen Y, Bradley KA, Zink JI, Nel AE. Differential expression of syndecan-1 mediates cationic nanoparticle toxicity in undifferentiated versus differentiated normal human bronchial epithelial cells. ACS Nano. 2011; 5(4):2756–2769. DOI: 10.1021/nn200328m [PubMed: 21366263]

Zhao XX, Heng BC, Xiong SJ, Guo J, Tan TTY, Boey FYC, Ng KW, Loo JSC. In vitro assessment of cellular responses to rodshaped hydroxyapatite nanoparticles of varying lengths and surface areas. Nanotoxicology. 2010; 5(2):182–194. DOI: 10.3109/17435390.2010.503943 [PubMed: 21609137]

Zhao X, Ng S, Heng BC, Guo J, Ma L, Tan TTY, Ng KW, Loo SCJ. Cytotoxicity of hydroxyapatite nanoparticles is shape and cell dependent. Arch Toxicol. 2012; in press. doi: 10.1007/s00204-012-0827-1

Ziolli RL, Jardim WF. Photocatalytic decomposition of seawater-soluble crude-oil fractions using high surface area colloid nanoparticles of TiO2. J Photochem Photobiol, A. 2002; 147(3):205–212.

Author Manuscript Author Manuscript Author Manuscript Author Manuscript

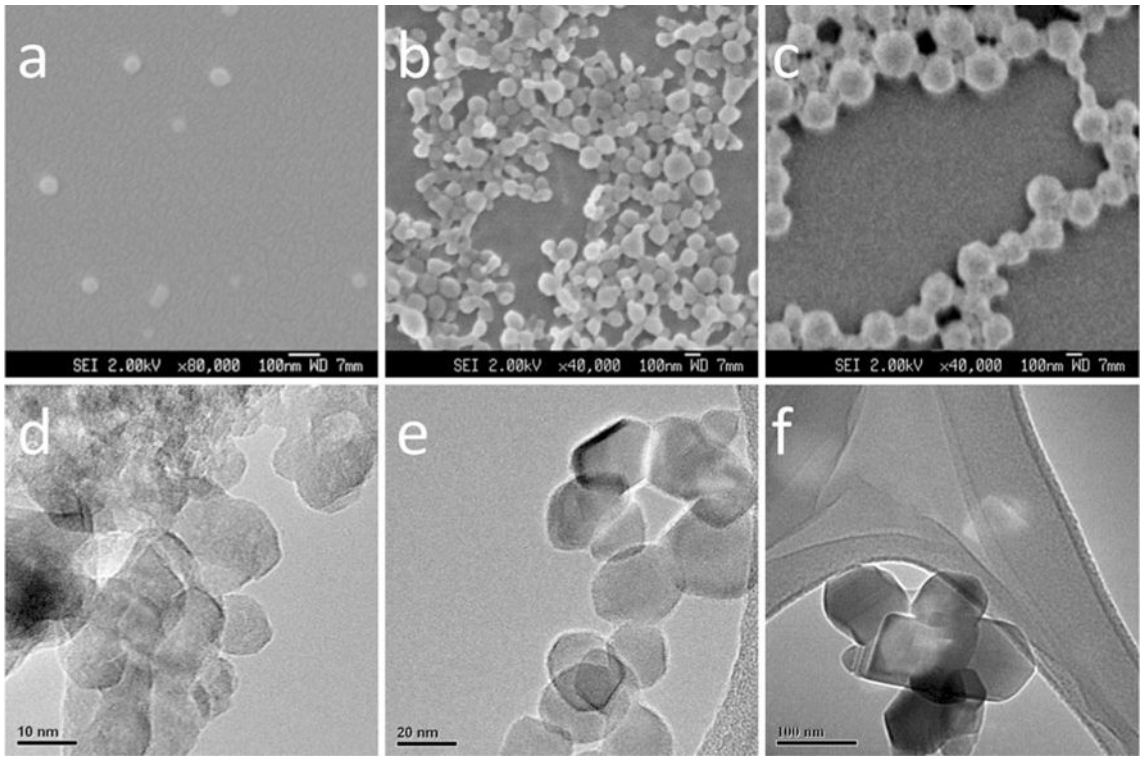


**Fig. 1.**

SEM micrographs of three spherical PLGA nanoparticle samples with different sizes **a** P60, PLGA nanoparticles of size 61 nm, *scale bar* 100 nm; **b** P100, PLGA nanoparticles of size 94 nm, *scale bar* 100 nm; **c** P200, PLGA nanoparticles of size 205 nm, *scale bar* 100 nm. TEM images of $TiO_2$ nanoparticles of three different sizes **d** T10, $TiO_2$ nanoparticles of size 10 nm, *scale bar* 10 nm; **e** T20, $TiO_2$ nanoparticles of size 20 nm, *scale bar* 20 nm; **f** T100, $TiO_2$ nanoparticles of size 100 nm, *scale bar* 100 nm

Author Manuscript Author Manuscript Author Manuscript Author Manuscript

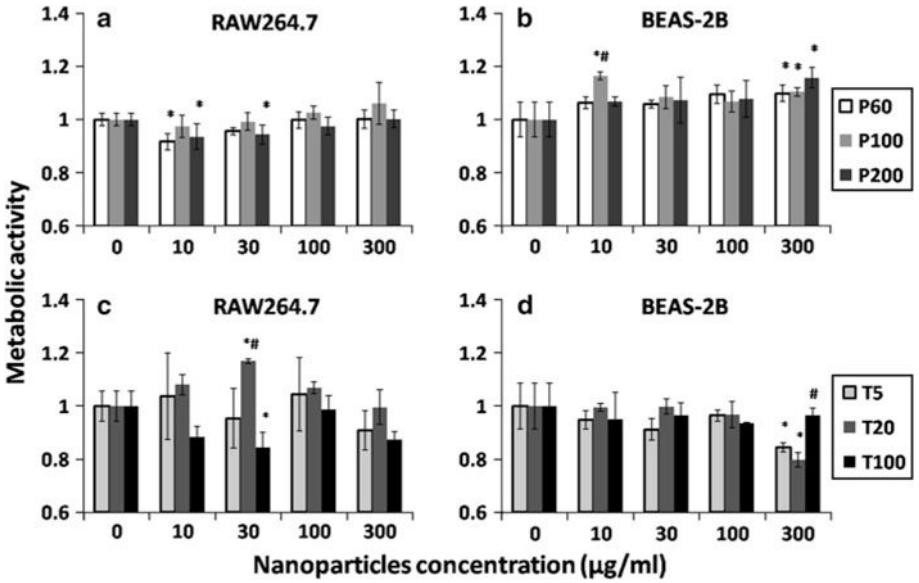


**Fig. 2.**

The metabolic activity of live cells after cells were incubated with PLGA and $TiO_2$ nanoparticles for 24 h. The metabolic activity of cells was quantified by MTS assay and normalized to negative control (0 μg/ml). **a** RAW264.7 cells after incubation with PLGA nanoparticles of three different sizes; **b** BEAS-2B cells after incubation with PLGA nanoparticles of three different sizes; **c** RAW264.7 cells after incubation with $TiO_2$ nanoparticles of three different sizes; **d** BEAS-2B cells after incubation with $TiO_2$ nanoparticles of three different sizes. The data represent mean ± SD, $n = 4$. *$p < 0.05$ compared with control (0 μg/ml). #$p < 0.05$ compared with other two particles in the same concentration

Author Manuscript Author Manuscript Author Manuscript Author Manuscript

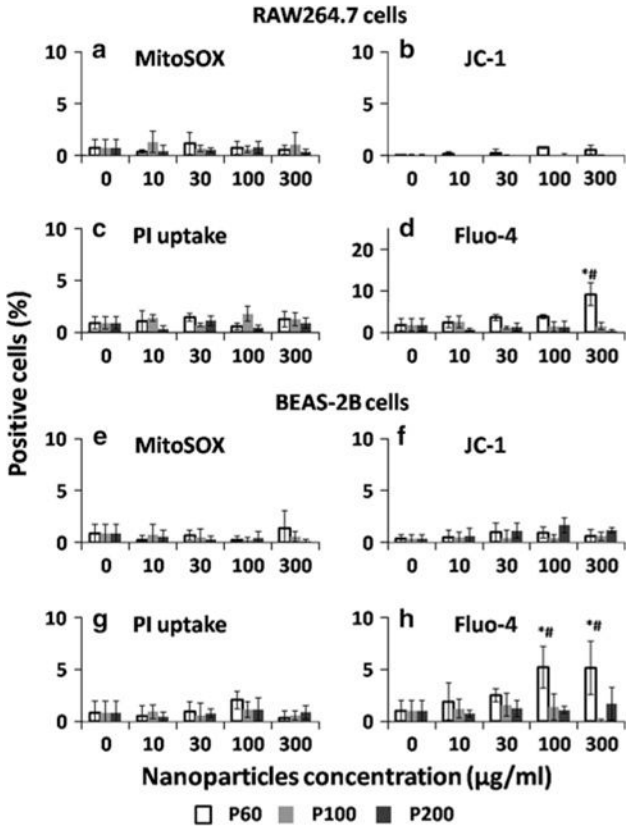


**Fig. 3.**

Multiparametric assays to detect the in vitro cytotoxicity of different-sized PLGA nanoparticles after 24 h incubation with (**a–d**) RAW264.7 and (**e–h**) BEAS-2B cells. The concentration ranges from 10 to 300 μg/ml. The cells were stained for 30 min with the dye cocktails to assay for (**a**, **e**) MitoSOX staining, (**b**, **f**) JC-1 staining, (**c**, **g**) PI uptake and (**d**, **h**) Fluo-4 staining. The percentage of cells showed positive fluorescence above a certain threshold was recorded by using Meta-Xpress software. The data represent mean ± SD, $n = 4$. *$p < 0.05$ compared with control (0 μg/ml). #$p < 0.05$ compared with other two particles in the same concentration

Author Manuscript Author Manuscript Author Manuscript Author Manuscript

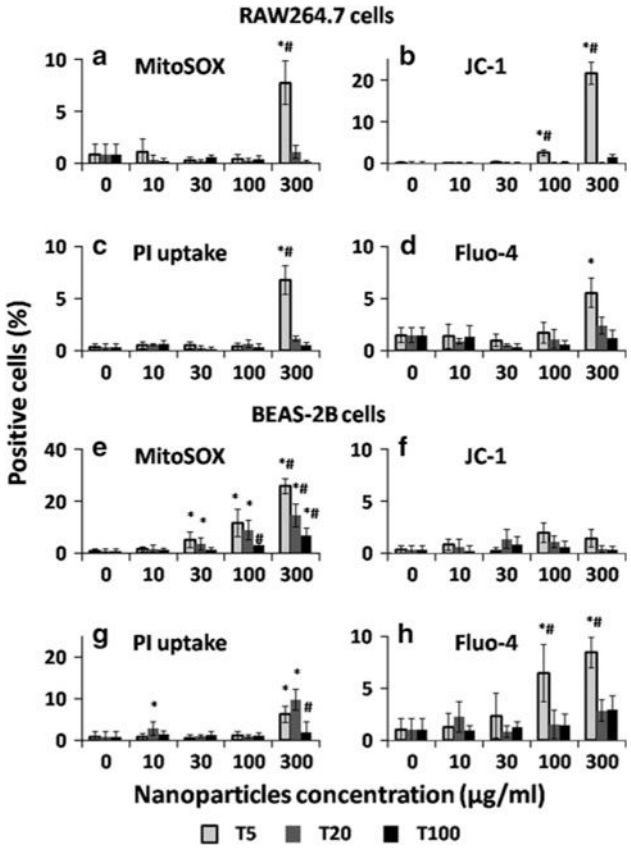


**Fig. 4.**

Multiparametric assays to detect the in vitro cytotoxicity of different-sized $TiO_2$ nanoparticles after 24 h incubation with (**a–d**) RAW264.7 and (**e–h**) BEAS-2B cells. The concentration ranges from 10 to 300 μg/ml. The cells were stained for 30 min with the dye cocktails to assay for (**a**, **e**) MitoSOX staining, (**b**, **f**) JC-1 staining, (**c**, **g**) PI uptake and (**d**, **h**) Fluo-4 staining. The percentage of cells showed positive fluorescence above a certain threshold was recorded by using Meta-Xpress software. The data represent mean ± SD, $n = 4$. *$p < 0.05$ compared with control (0 μg/ml). #$p < 0.05$ compared with other two particles in the same concentration

Author Manuscript Author Manuscript Author Manuscript Author Manuscript

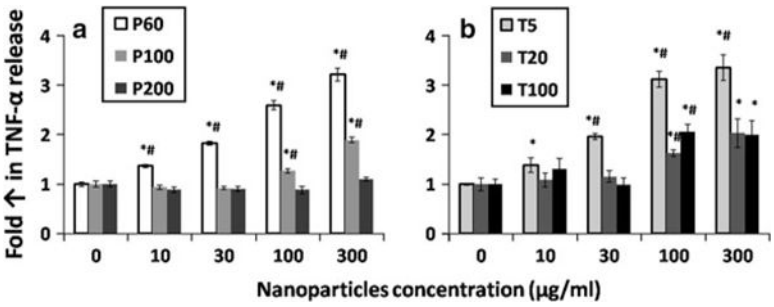


**Fig. 5.**

The TNF-α released from RAW264.7 cells after the cells were stimulated by **a** PLGA and **b** $TiO_2$ nanoparticles for 24 h. The TNF-α released from macrophages into medium was measured by ELISA and normalized to negative control (0 μg/ml). The data represent mean ± SD, $n = 4$. *$p < 0.05$ compared with control (0 μg/ml). #$p < 0.05$ compared with other two particles in the same concentration

Author Manuscript Author Manuscript Author Manuscript Author Manuscript

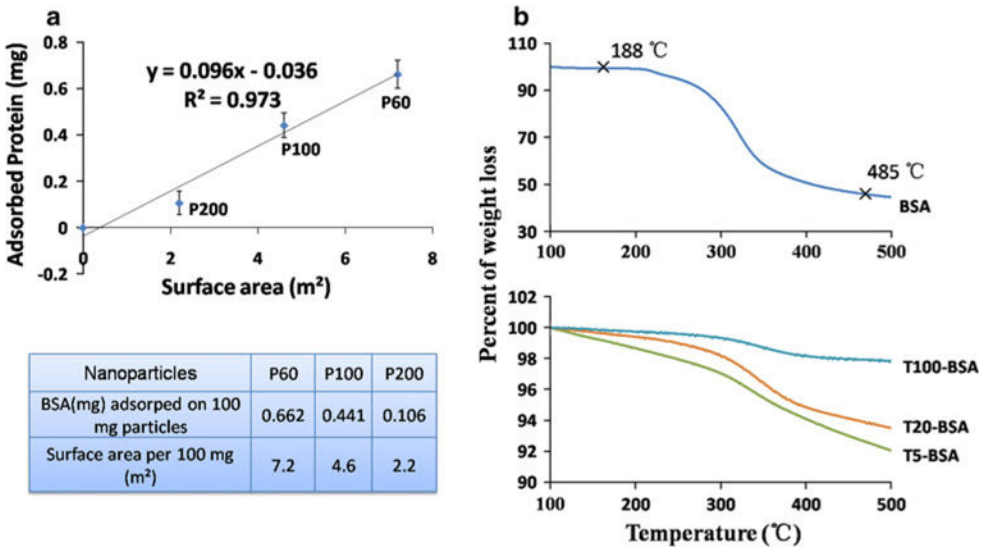


| Nanoparticles | P60 | P100 | P200 |
|---|---|---|---|
| BSA(mg) adsorped on 100 mg particles | 0.662 | 0.441 | 0.106 |
| Surface area per 100 mg ($m^2$) | 7.2 | 4.6 | 2.2 |

**Fig. 6.**

**a** Protein quantification of BSA attached on PLGA nanoparticles through Pierce 660 assay. The data represent mean ± SD, $n = 4$. **b** TGA analysis of BSA adsorption on $TiO_2$ nanoparticles. T10-BSA, T20-BSA and T100-BSA represent the weight decrease in particles after interaction with protein BSA. This indicated more BSA adsorbed onto T10 and T20 nanoparticles than on relatively larger T100 nanoparticles

Author Manuscript Author Manuscript Author Manuscript Author Manuscript

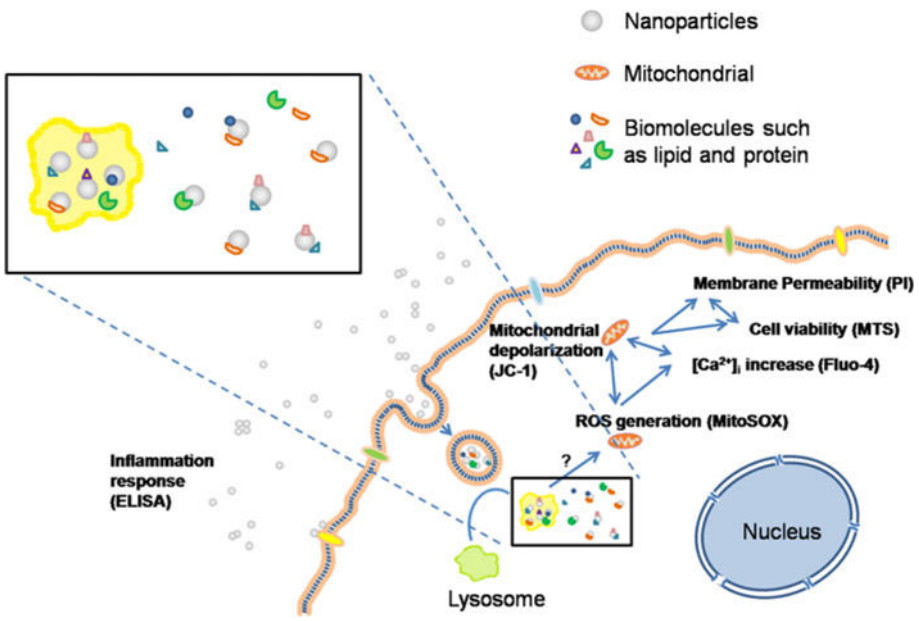


**Fig. 7.**

Schematic of the possible mechanism behind the size-dependent cytotoxicity of PLGA and $TiO_2$ nanoparticles

Author Manuscript

Author Manuscript

Author Manuscript

Author Manuscript

**Table 1**

Fluorescent probes used in this study

| Marker | Probe | Ex/em wavelength (nm) | Utility |
|---|---|---|---|
| Cell nucleus | Hoechst | 355/465 | Localization of cells |
| Plasma membrane damage | PI | 540/620 | Damaged integrity of plasma membrane |
| Mitochondrial superoxide | MitoSOX | 510/580 | Generation of mitochondrial superoxide |
| Mitochondrial membrane potential | JC-1 | 480/530–590 | Mitochondrial depolarization |
| Intracellular calcium | Fluo-4 | 480/510 | Increase in intracellular $Ca^{2+}$ concentration |

Author Manuscript Author Manuscript Author Manuscript Author Manuscript



**Table 2**

Characterization results of PLGA and $TiO_2$ nanoparticles with different particle sizes

| | | P60 | P100 | P200 | T10 | T20 | T100 |
|---|---|---|---|---|---|---|---|
| Primary particle size (nm) | | 61 | 94 | 205 | 10 | 20 | 100 |
| Water | Size (nm) | 101 | 149 | 207 | 669 | 307 | 349 |
| | PDI | 0.046 | 0.097 | 0.071 | 0.186 | 0.263 | 0.224 |
| | Zeta potential (mV) | −17.0 | −21.4 | −22.9 | −16.9 | 32.3 | 19.1 |
| CDMEM | Size (nm) | 192 | 120 | 196 | 262 | 338 | 444 |
| | PDI | 0.379 | 0.246 | 0.212 | 0.005 | 0.180 | 0.248 |
| | Zeta potential (mV) | −2.7 | −6.7 | −5.0 | −5.7 | −7.7 | −9.3 |
| BEGM | Size (nm) | 536 | 158 | 233 | 1,457 | 707 | 1,336 |
| | PDI | 0.343 | 0.131 | 0.110 | 0.298 | 0.289 | 0.255 |
| | Zeta potential (mV) | −6.4 | −9.6 | −3.6 | −11.0 | −12.1 | −9.9 |
| Theoretical surface area ($m^2$/g) | | 72 | 46 | 22 | 154 | 73 | 15 |
| BET surface area ($m^2$/g) | | / | / | / | 166.0 | 50.4 | 17.2 |
| Crystal structure | | / | / | / | Anatase | A*/R* 81/19 | Anatase |
| Endotoxin (EU/ml) | | <0.06 | <0.06 | <0.06 | <0.06 | <0.06 | <0.06 |

A* represents anatase

R* represents rutile